Volume 12, Number 1, 2019. pp. 7-15

Jordan Journal of Physics

ARTICLE

Comparative Study of Field Electron Emission from Single-Walled Carbon Nanotube and Multi-Walled Carbon Nanotube Mounted on Tungsten

Marwan S. Mousa, Samer I. Daradkeh and **Emad S. Bani Ali**

Surface Physics and Materials Technology Lab., Department of Physics, Mutah University, Al-Karak 61710, Jordan.

Received on: 2/7/2018; Accepted on: 26/11/2018

Abstract: Field Electron Emission (FEE) from Single-Walled Carbon Nanotubes (SWCNTs) and Multi-Walled Carbon Nanotubes (MWCNTs) mounted on blunt tungsten tip has been investigated to make sure that FEE comes from the CNTs. The FEE properties were studied using Field Emission Microscope (FEM), where the distance between the emitter and screen was fixed at ~10 mm and the system was evacuated to (~10^{-9} mbar). The emitters were prepared during two stages, with the first one being electrolytically etching the tungsten (W) wire of (0.1 mm diameter) in 2 mol of NaOH, while the second stage involves fixing the CNTs on the etched tungsten. Current-voltage (I-V) measurements were recorded and presented in the most common way as (I-V) plot with its related Fowler-Nordheim (FN) plot. It has been found that SWCNT samples have several advantages over MWCNT samples, such as the field electron emission having been initiated at lower applied voltage values and maintaining emitting electrons at lower applied voltage values, but MWCNTs emitted higher current values compared to SWCNTs.
Keywords: Field Electron Emission, SWCNTs, MWCNTs.

Introduction

Field electron emission (FEE) in solids occurs in intense electric field and is strongly dependent on the work function of the emitting material. In a parallel-plate arrangement, the macroscopic field E_{macro} between the plates is given by $E_{macro} = V/d$, where d is the plate separation and V is the applied voltage. If a sharp object is created on a plate, then the local field E_{local} at its apex is greater than E_{macro} and can be related to E_{macro} by [1]:

$$E_{local} = \gamma \times E_{macro} .$$

The parameter γ is called the field enhancement factor and is basically determined by the shape of the object [1]. FEE occurs when the applied electric field value is ~ 10^9 V/m [2]. In order to achieve that high electric field at the tip of a sample, the sample has been fabricated to have a high tip curvature [3].

Metals have been extensively used as field electron emitters until 1991, where Multi-Walled Carbon Nanotube (MWCNT) was discovered accidentally by Sumio lijima [4] while studying the surfaces of graphite electrode used in electric arc discharge. Two years later, Single-Walled Carbon Nanotube (SWCNT) was discovered by the same scientist and his colleagues [5]. These materials have attracted much attention due to their features, so they can be used as field electron emitters [6].

Carbon materials exist in various forms, such as graphite, diamond, carbon fibers, fullerenes and carbon nanotubes. Carbon nanotubes show distinguished properties and their discovery had

Corresponding Author: Marwan S. Mousa **Email**: mmousa@mutah.edu.jo

a great impact on the development in the field of semiconductor science due to their unique properties [7]. Those tubes are considered to be the strongest and stiffest materials yet discovered in terms of tensile strength and elastic modulus, because of the covalent sp^2 bonds formed between individual carbon atoms [8], electrical properties [9], mechanical strength and chemical strength [10]. The natural resonance (fundamental vibrational frequency) of a cantilevered single-wall nanotube of 1 micron length is shown to be about 12 MHz [11]. It is one of the best candidates to be used as field electron emitters because of the advantages it has over other metallic emitters, such as enhanced current stability, low threshold voltage, nano-size, high aspect ratio and long lifetime [12]. Due to these properties, CNTs are very widely used in technological and industrial fields, such as flat panel displays, cathode-ray-tube lighting elements and drug delivery systems [13].

Field emission behavior of a CNT strongly depends upon its morphology, diameter, alignment and the contact between the CNT and the substrate, as well as the condition of the CNT tip (defects, adsorption, doping, … and so on) [14]. The FN theory can reveal some basic factors that have influence on the FE mechanism. The experimental data can reveal other factors, such as value of the enhancement factor and emitting area [15]. The best method to represent the experimental data is using the FN plot, $ln(I/V^2)$ vs. $1/V$, and the expected shape of the FN plot is a straight line according to the theory. However, experimentalists experienced a deviation from FN theory during testing the FE mechanism from CNTs, that could be as an effect of non-uniform field enhancement factor [16], or adsorbed molecules, influence of high apex curvature, space charge effect, localized electron state, contact resistance, among others [17]. The main aim of this article is to keep the ongoing research of seeking for optimum field emission (FE) cold cathodes by studying and comparing the two kinds of CNTs employed in this investigation. In previous research, FE differences between FEE from SWCNTs and MWCNTs have been investigated, where both emitters have been prepared using different preparation techniques from the preparation technique mentioned in [18]. Variation in results was obtained due to these differences; so critical comparison between the results reported here and those previously found [19] will be carried out in the future. In this study, it can be noted that a SWCNT emitter can initiate electron emission at lower applied voltage values, but an MWCNT emitter produces a higher electron emission current than that from an SWCNT emitter [19].

Materials and Methodolgy

This study uses SWCNTs produced by catalytic conversion of high-pressure Carbon Monoxide over Fe particles (HiPCO) processed at CNI, Houston, TX, where the length of individual SWCNT is approximately (1 - 3) μm and the mean diameter is (1 - 4) nm. The MWCNT Nanocly^{TM} NC 7000 of a carbon purity of (90%) and an average tube diameter of (9.5 nm) with high aspect ratio (> 150) has been tested. In the etching process, a tungsten wire of (0.1 mm) diameter and high purity (99.95 %) was used (Produced by Good Fellow Metals Company, UK).

The emitters were fabricated by mounting the CNTs over a blunt tungsten tip, to make sure that the tungsten (W) does not contribute to the field emission process. The mounting procedures consisted of two steps; the first step starts with preparing the tungsten substrate using electrolytic etching of a wire at the meniscus of a 2 mol/liter of NaOH solution; i.e., by same technique used for tungsten emitters [20-21]. Etching process starts with cutting ~3 cm of tungsten wire, then attaching one of its ends inside a stainless steel tube. The tungsten wire has been etched using an electrochemical circuit, using a power supply (10 – 12 V), an ammeter and a graphite rod as a cathode. The process has been performed in Pyrex glass beakers that are connected by a separating glass pipe to prevent interfering of the produced hydrogen in the etching process [22]. By immersing about 0.3 cm of the W wire in the etching NaOH solution, the electrical etching process starts. This process ends by removing the tungsten from the NaOH solution, after the etching current suddenly drops. Fig. 1 shows a schematic diagram of the electrical etching circuit.

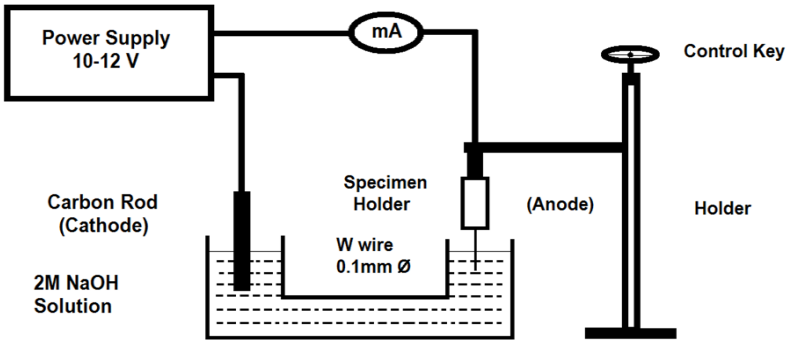

FIG. 1. Schematic diagram of electrical etching circuit.

After ultrasonic cleaning for ~8 min, we start with the second step which involves applying a thin layer of epoxylite resin; that is necessary to attach the CNT over the tungsten tip. The tungsten blunt tip was slowly and regularly dipped once into the epoxy resin, then very slowly pulled out to prevent the formation of bubbles [23]. Then, the CNTs were mechanically attached to the tungsten tip under observation of optical microscopy.

In the work reported here, various types of CNTs/W blunt emitters have been characterized using the conventional field electron microscope (FEM) with tip-screen separation standardized at 10 mm. The vacuum system was baked out at ~170 °C overnight having a pressure during the FEE tests of ~ 2×10^{-9} mbar. The most common method of investigating the emitter behavior is recording the current-voltage (I-V) characteristics and presenting the data produced as I-V as well as FN plots [24].

Generally, Fowler-Nordheim (FN) theory has been employed to describe field emission behavior of metals. The theory is expressed by the following equation [25]:

$$I = \lambda A a \phi^{-1} F^2 \exp\left(-\mu b \phi^{3/2}/F\right)$$

where ϕ and F are the local work function and the barrier field, a and b are the usual universal FN constants, A is the emission area and λ and μ are the generalized correction factors.

Results

Fig. 2 presents SEM images for both types of emitters, where the attached CNTs on the tungsten blunt tips are shown (SWCNTs on blunt W tip (left) and MWCNTs on blunt W tip (right)). Attaching CNTs on iron tip has been done by [26] and MWCNTs on tungsten tip by [26-27] in order to study the FEE from these CNTs. In this work, we will investigate the FEE mechanism from SWCNTs on blunt tip and MWCNTs on blunt tungsten tip.

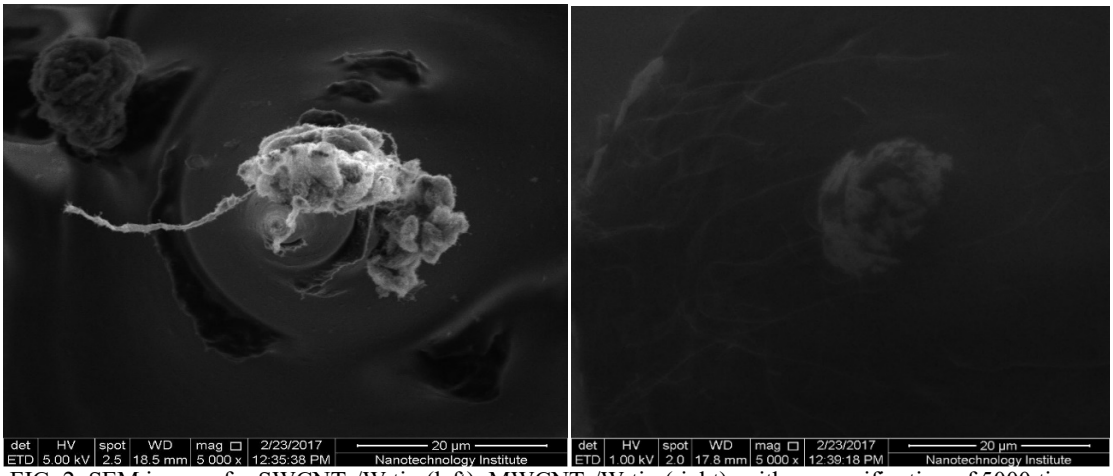

FIG. 2. SEM images for SWCNTs/W tip (left), MWCNTs/W tip (right), with a magnification of 5000 times.

As mentioned before, we attached the CNTs on blunt tungsten tip, in order to make sure that tungsten tip will not contribute to the FEE process.

We performed the tests on the two types of samples, (SWCNTs/W) and (MWCNTs/W), under the same conditions. The voltage applied to the SWCNTs/W tip was slowly increased with the I-V characteristics being recorded. The emission current initiated at 2 pA with the applied voltage at 450 *V*. The emission current increased linearly by increasing the applied voltage, thus indicating a constant-resistance regime. Then, the applied voltage has been increased until "switch-on" phenomenon occurs at (V_{SW}=1250 V). The emission current was suddenly raised from nA range to µA range, where the emission current was (2.9 µA). By further increasing the applied voltage, the emission current continued increasing, until (2850 V) was reached, where the recorded emission current was (17.9 µA). By decreasing the applied voltage, the linear region of the FN plot extends down to (V = 650 V), with an emission current (I = 1.06 µA). By further voltage decreasing, the emission current vanishes at (V_{TH} = 400 V), with an emission current (I_{TH} = 3 pA). Fig. 3 shows the I-V characteristics and the related FN plots for (SWCNTs/W). The slope of both voltage cycles is pointed out in the FN plots (for low emission current value), where the slope of FN plot can reveal the value of some important parameters like field enhancement factor by calculating the slope and emission area through calculating the intercept [28].

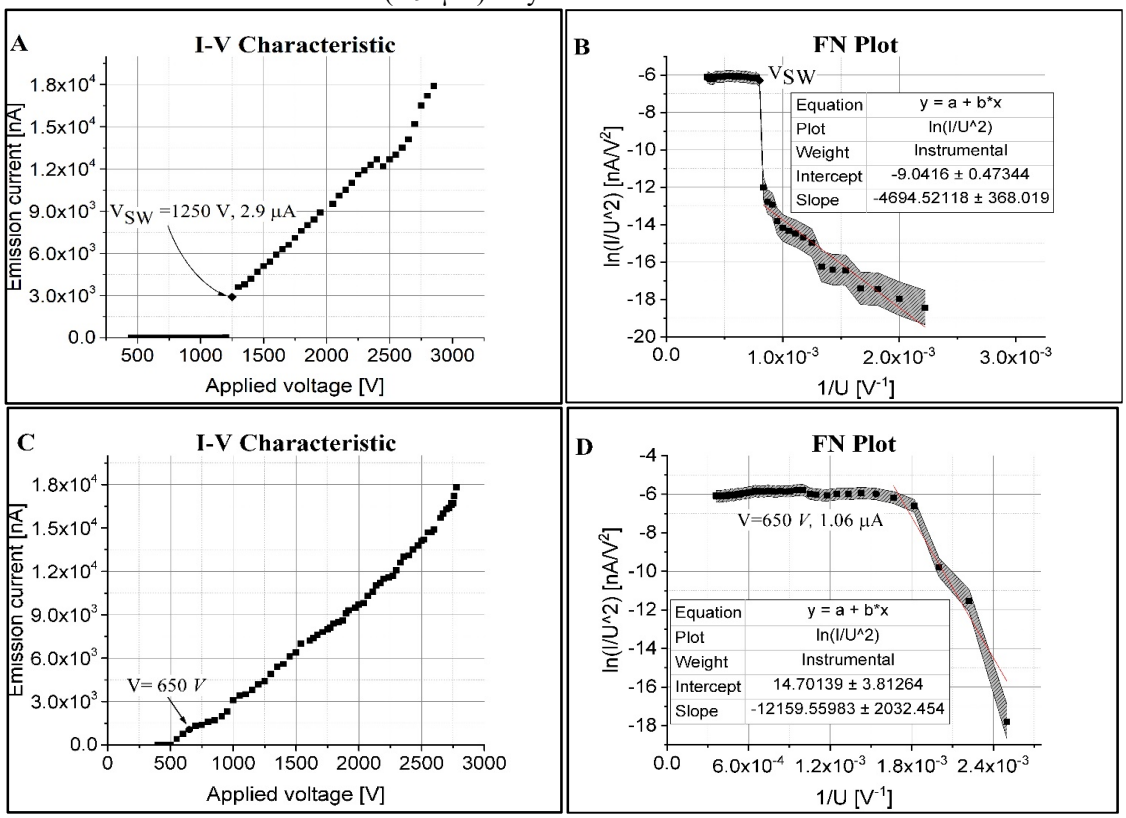

FIG. 3. (SWCNTs/W): at increasing voltage - (A) I-V characteristics and (B) FN plot. At decreasing voltage - (C) I-V characteristics and (D) FN plot.

As it appeared from Fig. (3-B and D), there are multi-linear segment FN plots, which can be divided into two linear segments. Such behavior could be attributed to the existence of constant resistance. The indication of the existence of constant resistance is the linear increase in the I-V plot in Fig. (3A). Additionally, the slope value for the increasing cycle of the applied voltage is -4694.5 Np, while the decreasing voltage cycle gave a slope of -12159.5 Np.

For the (MWCNTs/W) emitter, at an applied voltage value of 750 V, the emission current with a value of 9.4 pA has been initiated. By further increasing the applied voltage, the

emission current increased until the applied voltage reached (3920 V), where "switch-on" phenomenon suddenly occurred with an emission current value of (22 μA) recorded. It is to be noted that the emission current increased from 6.3 nA to 22 μA. By decreasing the applied voltage, the emission current started to decrease, but it remained in the (μA) range until the applied voltage reached (V = 1000 V), where the emission current was (I = 2.1 μA). As being noted from Fig. 4, the linear behavior appeared in the I-V characteristics of the MWCNTs, where it has the same indication, illustrating the existence of constant resistance. By further decreasing the applied voltage, the emission current continues to decrease until it vanishes at (V_{TH} = 670 V), (I_{TH} = 8.2 pA). Fig. 4 shows the I-V characteristics and the related FN plot, with the slope shown by the FN plots (for low emission current). The FN plot that is related to FEE from MWCNTs shows a multi-linear segment as the FN plot of SWCNTs, which could be the same evidence for the existence of constant resistance. In addition, the FN plot shape bends downward at its left end which indicates an increasing field enhancement factor [29]. From the FN plots for FEE from MWCNTs (Fig. 4), the slope values at increasing and decreasing cycles of the applied voltage are -18204.4 Np and -18649.9 Np, respectively.

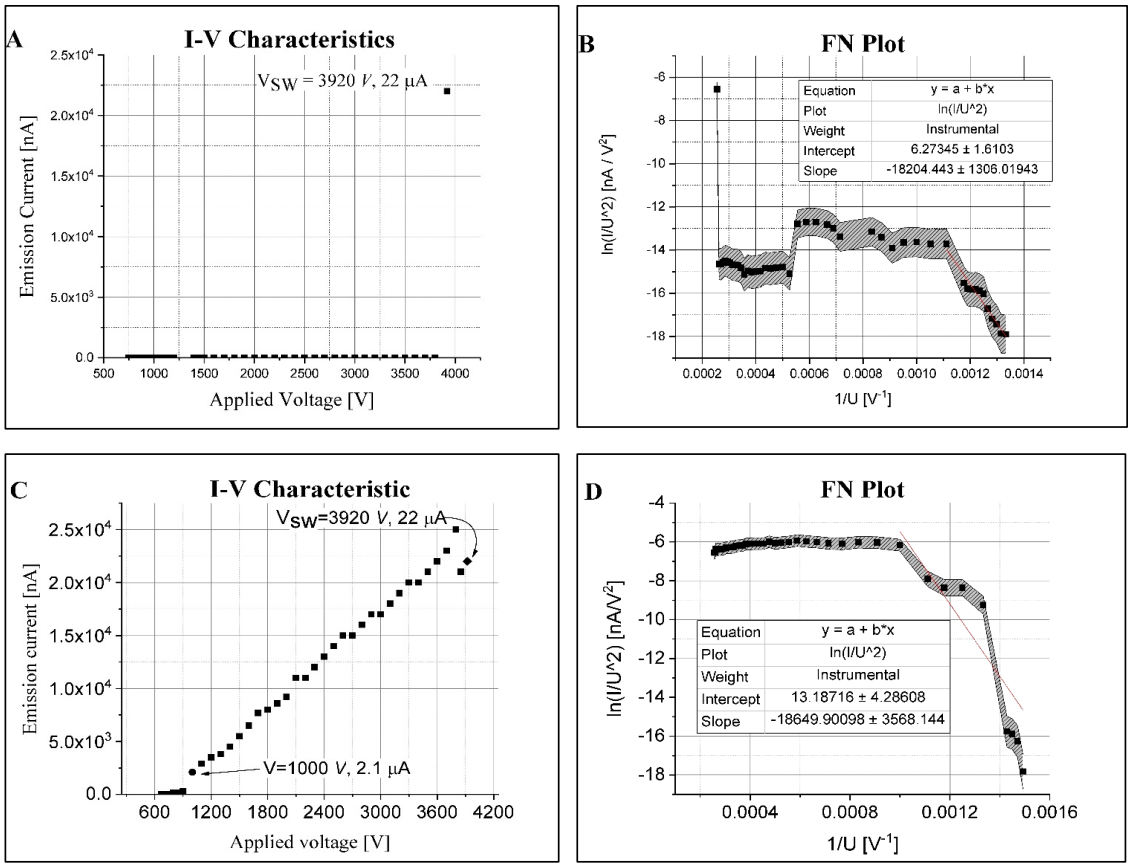

FIG. 4. (MWCNTs/W): at increasing voltage - (A) I-V characteristics and (B) FN plot. At decreasing voltage - (C) I-V characteristics and (D) FN plot.

The experiments were repeated under the same conditions. For the (SWCNTs/W) emitter, the applied voltage ranged between (550 V) and (1400 V), with an emission current of (9 pA) to (4.2 μA) recorded, with the "switch-on" phenomenon occurring at (V_{SW} =1000 V), (I_{SW} = 1.3 μA). The emission current increased linearly at an applied voltage of (900 V) to (1400 V), then with starting to decrease the applied voltage, the linear region extends from (V = 1350 V), (I = 4.1 μA) to (V= 500 V), (I= 70 nA). By further decreasing the applied voltage, the emission current falls smoothly to (I_{TH} = 1 pA), where the applied voltage value was (V_{TH} = 300 V). Fig. 5 shows the I-V characteristics and related FN plot at increasing and decreasing voltage.

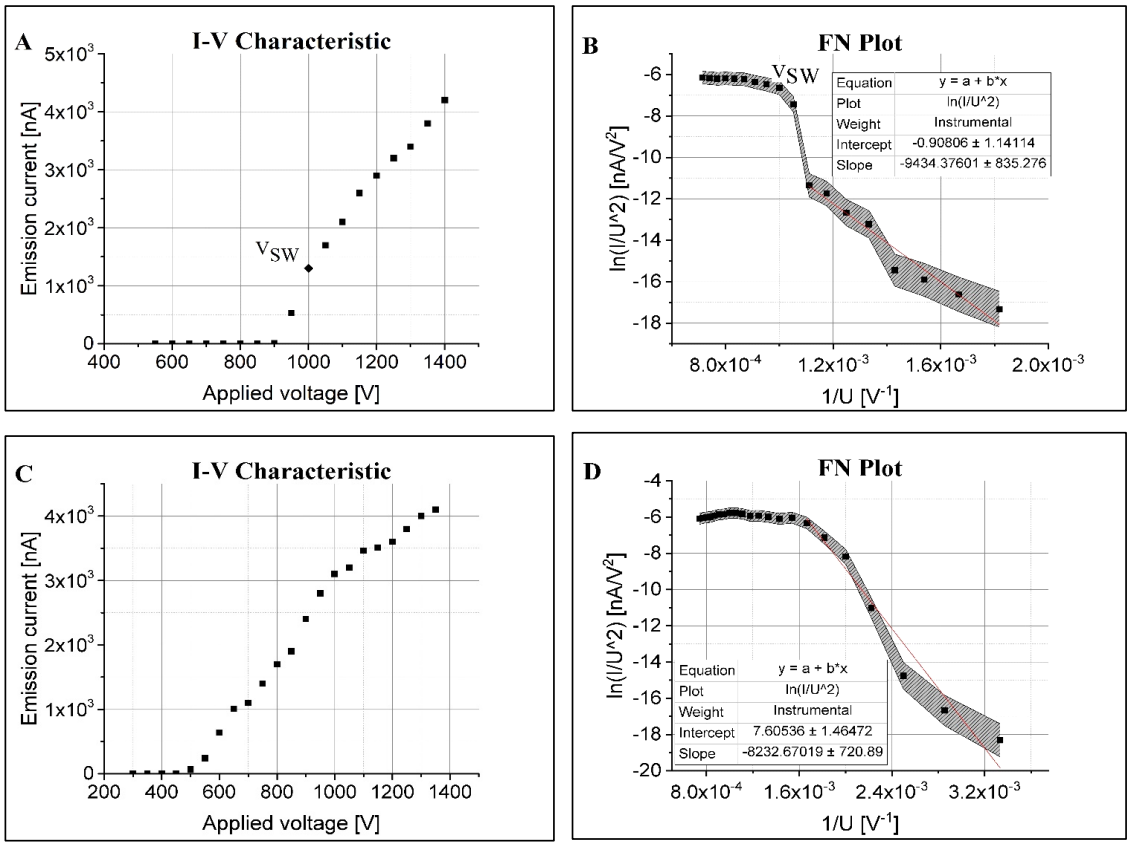

FIG. 5. For (SWCNTs/W). Cycle 2; at increasing voltage - (A) I-V characteristics and (B) FN plot. At decreasing voltage - (C) I-V characteristics and (D) FN plot.

In case of (MWCNTs/W) emitter, the applied voltage ranges from (800 V) to (1930 V), with an emission current ranging from (9 pA) to (6.1 μA), where the "switch-on" phenomenon occurs at an applied voltage value of (V_{SW} = 1930 V), with an emission current value of (I_{SW} = 6.1 μA). During the decreasing cycle ranging from (1930 V) to (560 V), with an emission current ranging from (6.1 μA) to (7 pA), the saturation region extends down to (V_{SAT} = 1250 V), with the emission current value (I_{SAT} = 1.1 μA) and by further decreasing the applied voltage, the emission current vanishes at (V_{TH} = 560 V) with (I_{TH} =7 pA). Fig. 5 shows the I-V characteristics and related FN plot for the (SWCNTs/W) emitter, while Fig. 6 shows the I-V characteristics and related FN plot for the (MWCNTs/W) emitter. The slope values of the FN plot that relates to SWCNT emitter at low emission current value during the increasing and decreasing voltage cycles are -9434.37 Np and -8232.67 Np, respectively. The slope values of FN plot that relates to MWCNT emitter at low emission current value at increasing and decreasing applied voltage are -1114.63 Np and -12643 Np, respectively. Fig. 7 shows a set of emission current images for (SWCNT/W) and (MWCNT/W).

From Fig. 7, it can be seen that the emission current image of the SWCNT emitter is more concentrated than the emission current image of the MWCNT emitter at V_{SW} value. Also, the emission current value at V_{SW} of MWCNT emitter is higher than that of SWCNT emitter.

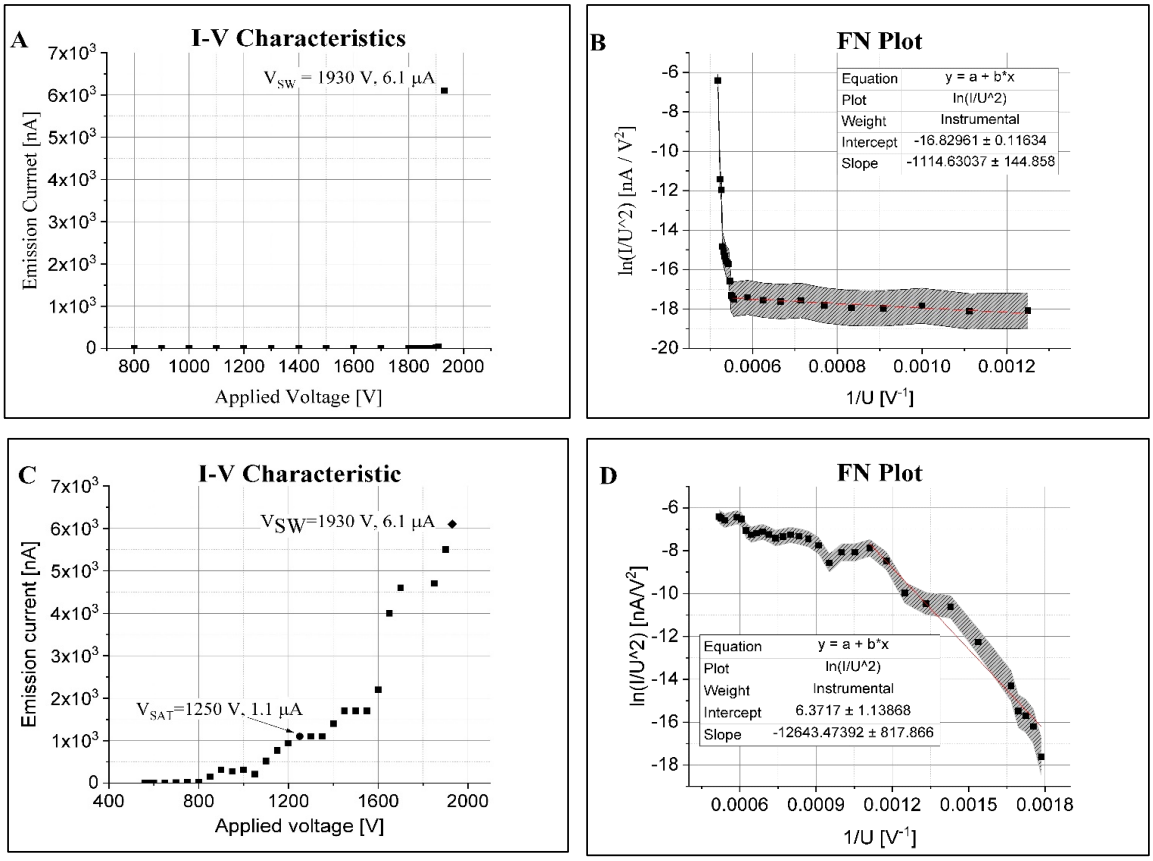

FIG. 6. For (MWCNTs/W). Cycle 2; at increasing voltage - (A) I-V characteristics and (B) FN plot. At decreasing voltage - (C) I-V characteristics and (D) FN plot.

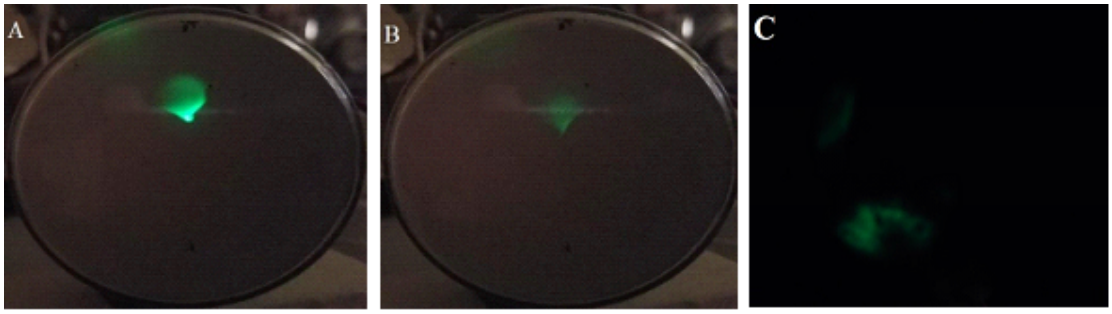

FIG. 7. Emission images at applied voltage (SWCNTs/W) (A) V_{SW} =1250 V, I_{SW} =2.9 µA. (B) V_{SAT} =650 V, I_{SAT} =1.06 µA. (MWCNTs/W) (C) V_{SW}= 1930 V, I_{SW}=6.1 µA.

By comparing the slope value for the (SWCNTs/W) emitter with that of the (MWCNTs/W) emitter, according to [30], the slope value from the FN plot S is given as:

$$S = -6.44 \times 10^9 \times \phi^{3/2}(d/\gamma);$$

where S is the slope value from FN plot, ϕ is the effective work function, d is the diameter of the CNT and γ is the field enhancement factor. According to the previous equation, it can be found that the field enhancement factor value for (SWCNTs) is higher than that for (MWCNTs). This indicates that the field concentration at (SWCNT) emitter tip is higher than that in the case of (MWCNT) emitter. This can cause a reduction of the effective threshold voltage for emission [31].

It can be seen from the SEM images of (SWCNTs/W) and (MWCNTs/W) that the CNTs are not perfectly vertically aligned on the

tungsten tip. Vertically aligned CNTs are better than randomly aligned CNTs on tungsten tip, where the field enhancement factor in case of vertically aligned CNTs will be higher than for randomly aligned CNTs on tungsten tip [32]. The lower the number of CNTs mounted on tungsten tip, the higher the field enhancement factor value will be, because having a lower number of neighboring tubes will reduce the screening effect [33-34], but the emission current density will be lower due to lower active emission area.

Conclusions

The emission current behavior has been recorded during increasing and decreasing cycles of the applied voltage on the emitter surface in order to obtain the FN plots. FN plots for both emitters have shown that the SWCNT emitter has a higher field enhancement factor, which is the reason behind the lower recorded value of the "switch-on" voltage, lower saturation region value and lower threshold voltage. For the SWCNT emitter, the "switch-on" phenomenon occurs at lower applied voltage value than that for the MWCNT emitter. Also, the saturation region extends down to lower voltage values in the case of SWCNT emitter than that in the MWCNT emitter. But, the MWCNT emitter can emit a higher emission current than that emitted from the SWCNT emitter. From the I-V characteristics of the first cycle of increasing and decreasing of the applied voltage for both SWCNTs and MWCNTs (Figs. 3 and 4), it can be seen that the shape of I-V characteristics has a linear trend, that indicates the existence of a constant resistance somewhere at the CNT/substrate interface or along of the CNT.

In the future, a more accurate methodology will be used to mount the CNTs on the metallic base using nano-manipulator. This will enable to create more accurate uniformly aligned CNTs on metal substrates and create large-area field electron emitter (LAFE) of CNTs to compare its FEE characterization with that an individual CNT emitter. All of the above is for maintaining the ongoing research aiming at obtaining the optimum field electron emitter.

Acknowledgments

The authors would like to thank the Deanship of Academic Research at Mu'tah University for supporting this work through research project number 241/19/120.

References

[1] Lan,Y., Wang, Y. and Ren, Z.F., Advances in Physics, 60 (4) (2011) 553.

[2] Latham, R.V. and Mousa, M.S., Journal of Physics D: Applied Physics, 19 (4) (1986) 699.

[3] Yunhan, L., Yonghai, S. and Yeow, J.T.W., Nanotechnology, 26 (24) (2015) 242001.

[4] Iijima, S., Nature, 354 (6348) (1991) 56.

[5] Iijima, S. and Ichihashi, T., Nature, 363 (6430) (1993) 603.

[6] Heo, S., Ihsan, A., Yoo, S., Ali, G. and Cho, S., Nanoscale Research Letters, 5 (4) (2010) 720.

[7] Nasir, S., Hussein, M.Z., Zainal, Z. and Yusof, N.A., Materials, 11 (2) (2018) 295.

[8] Yu, M.-F., Lourie, O., Dyer, M.J., Moloni, K., Kelly, T.F. and Ruoff, R.S., Science, 287 (5453) (2000) 637.

[9] Popov, V.N., Materials Science and Engineering: R: Reports, 43 (3) (2004) 61.

[10] Peng, S., O'Keeffe, J., Wei, C., Cho, K., Kong, J., Chen, R., Franklin, N. and Dai, H., Carbon Nanotube Chemical and Mechanical Sensors. In: International Workshop on Structural Health Monitoring, (2001) 1-8.

[11] Ruoff, R.S. and Lorents, D.C., Carbon, 33 (7) (1995) 925.

[12] Hong, P.N., Thang, B.H., Hong, N.T., Lee, S. and Minh, P.N., Journal of Physics: Conference Series, 187 (2009) 012041.

[13] Bianco, A., Kostarelos, K. and Prato, M., Current Opinion in Chemical Biology, 9 (6) (2005) 674.

[14] Evtukh, A., Hartnagel, H., Yilmazoglu, O., Mimura, H. and Pavlidis, D., "Vacuum Nanoelectronic Devices: Novel Electron Sources and Applications". (John Wiley and Sons, United Kingdom, 2015).

[15] Liang, S.-D., "Quantum Tunneling and Field Electron Emission Theories". (World Scientific Publishing Co. Pte. Ltd., 2013) 1-387.

[16] Lu, X., Yang, Q., Xiao, C. and Hirose, A., Journal of Physics D: Applied Physics, 39 (15) (2006) 3375.

[17] Kleshch, V.I., Eremina, V.A., Serbun, P., Orekhov, A.S., Lützenkirchen-Hecht, D., Obraztsova, E.D. and Obraztsov, A.N., Physica Status Solidi (B), 255 (1) (2018) 1700268.

[18] Bani-Ali, E. and Mousa, M.S., Applied Microscopy, 46 (2016) 244.

[19] Mousa, M.S., IOP Conference Series: Materials Science and Engineering, 305 (1) (2018) 012025.

[20] Müller, E.M., Zeitschrift für Physik, 106 (1937) 541.

[21] Mousa, M.S., Surface Science, 266 (1-3) (1992) 110.

[22] Revenikiotis, A., "Optimization of STM-Tip Preparation Methods". (Royal Institute of Technology (KTH), Stockholm, Sweden, 2010).

[23] Mousa, M.S., Surface Science, 231 (1) (1990) 149.

[24] Forbes, R., Deane, J., Fischer, A. and Mousa, M., Jordan J. Phy., 8 (2015) 125.

[25] Forbes, R.G., Deane, J.H.B., Hamid, N. and Sim, H.S., Journal of Vacuum Science and Technology B: Microelectronics and Nanometer Structures Processing, Measurement and Phenomena, 22 (3) (2004) 1222.

[26] Zhong, D.Y., Zhang, G.Y., Liu, S., Sakurai, T. and Wang, E.G., Applied Physics Letters, 80 (3) (2002) 506.

[27] Pasquini, A., Picotto, G.B. and Pisani, M., Sensors and Actuators A: Physical, 123-124 (2005) 655.

[28] Fischer, A., Mousa, M.S. and Forbes, R.G., Journal of Vacuum Science and Technology B, 31 (3) (2013) 032201.

[29] Wang, W. and Li, Z., Mesoscale and Nanoscale Physics, 2012.

[30] Cheng, T.C., Chen, P.Y. and Wu, S.Y., Nanoscale Research Letters, 7 (1) (2012) 125.

[31] Peng, J., Li, Z., He, C., Deng, S., Xu, N., Zheng, X. and Chen, G., Physical Review B, 72 (23) (2005) 235106.

[32] Cheng, Y. and Zhou, O., Comptes Rendus Physique, 4 (9) (2003) 1021.

[33] Suh, J.S., Jeong, K.S., Lee, J.S. and Han, I., Applied Physics Letters, 80 (13) (2002) 2392.

[34] Cai, D. and Liu, L., AIP Advances, 3 (12) (2013) 122103.